Effective Screening of Hydrodynamic Interactions in Charged Colloidal Suspensions

Dirk O. Riese,[1] Gerard H. Wegdam,[1] Willem L. Vos,[1] Rudolf Sprik,[1]
Denis Fenistein,[1] Jeroen H. H. Bongaerts,[1] and Gerhard Grübel[2]

[1]*Van der Waals-Zeeman Instituut, Universiteit van Amsterdam, Valckenierstraat 65-67, 1018 XE Amsterdam, The Netherlands*

[2]*European Synchrotron Radiation Facility, BP 220, 38043 Grenoble, France*

(Received 17 February 2000)

We investigate the hydrodynamic interaction in suspensions of charged colloidal silica spheres. The volume fraction as well as the range of the electrostatic repulsion between the spheres is varied. Using a combination of dynamic x-ray scattering, cross-correlated dynamic light scattering, and small angle x-ray scattering, the hydrodynamic function $H(q)$ is determined experimentally. The effective hydrodynamic interactions are found to be screened, if the range of the direct interaction is relatively long and the static density correlations are strong. This observation of effective hydrodynamic screening is in marked contrast to hard-sphere-like systems.

PACS numbers: 82.70.Dd, 61.10.–i

Colloidal suspensions have intriguing static and dynamic properties due to their composite nature and the mesoscopic length scales involved. Colloids interact by direct forces, such as electrostatic or hard-sphere repulsions, and hydrodynamic forces mediated by the suspending fluid [1,2]. Whereas the static properties of colloidal suspensions are strikingly similar to those of molecular fluids, the important role of the suspending medium leads to significant differences in the dynamical behavior. The complex viscoelastic and diffusional properties of colloidal suspensions depend on the interplay between direct and hydrodynamic interactions. This interplay is governed by the ratio of the different length scales in the system [3], such as particle radius, interparticle distance, and the range of the interactions. Unraveling these fascinating effects is challenging from a fundamental point of view and allows us to tailor the characteristics of colloidal suspensions for technological applications.

The hydrodynamic interaction between two isolated particles is long range, since it decays with the inverse of the interparticle distance [1,2]. An open question is whether many-body effects in colloidal suspensions can result in screening of the bare hydrodynamic interaction, leading to an *effective* pair interaction that is no longer long range. The concept of hydrodynamic screening is vigorously being discussed in the context of sedimentation [4], where several possible screening mechanisms have been proposed [5]. Recently, it has been shown theoretically that hydrodynamic interactions are partially screened for particles on a lattice [6]. Screening of the hydrodynamic velocity field also occurs in porous media, where the solid frame remains fixed [7]. A phenomenologically similar effect is known from polyelectrolyte solutions, where the coupling of electrostatic and hydrodynamic interactions between the chain segments leads to *apparent* hydrodynamic screening [8]. The most successful theory for the hydrodynamic interactions in dense colloidal suspensions to date, known as the fluctuation expansion, has been developed by Beenakker and Mazur [9]. Their theory, which includes many-body hydrodynamic interactions in an approximate way, does not involve screening. The theory has been confirmed in the case of hard-sphere-like colloids [10] and has also been applied successfully to slightly charged colloids at moderate volume fractions [11]. Later, Nägele and co-workers developed a simpler, pairwise additive (PA) theory [2]. The PA theory is adequate at low [12] to moderate volume fractions [2,13]. The work on charged colloidal suspensions has been reviewed by Nägele [2]. As he points out [2,14], many-body hydrodynamic effects become noticeable at volume fractions above about 10% and one has to resort to the elaborate fluctuation expansion in this concentration regime. To date, there are very few experimental data on concentrated charged colloidal suspensions [13]; it is this region of dense charged colloidal dispersions we address in this paper.

We report the first experimental observation of effective hydrodynamic screening in charged colloidal suspensions. We use a unique combination of dynamic x-ray scattering (DXS), cross-correlated dynamic light scattering (CCDLS), and small angle x-ray scattering (SAXS). This new combination of techniques is cardinal to obtain the collective diffusion coefficient *and* the static structure factor simultaneously, free from multiple scattering effects, over a sufficiently wide range of wave vectors. This allows us to determine the hydrodynamic function on optically strongly scattering samples purely experimentally, free from any modeling of the dynamic or static properties. The multiple-scattering free experimental techniques used give us complete freedom to change the properties of the solvent and thus vary the range and strength of the electrostatic repulsion between the colloids. Doing so, we observe a strong influence of the structure on the hydrodynamic interactions. For samples with relatively weak interparticle structuring, the data agree reasonably well with fluctuation expansion calculations [9]. As the range of the direct interaction increases and static density correlations

 0031-9007/00/85(25)/5460(4)$15.00

become stronger, however, we find large deviations from this theory. Our results show that higher-order many body effects in dense, charge stabilized colloidal suspensions, that are beyond the scope of current theories, lead to a flattening of the hydrodynamic function [see Fig. 3]. Phenomenologically, this flattening can be described as hydrodynamic screening. To our knowledge, this or similar effects have not been reported before.

We used colloidal silica spheres (mean radius $a = 54.9 \pm 0.1$ nm, polydispersity $\sigma = 0.042 \pm 0.005$, density $\rho = 1.93 \pm 0.03$ g/cm^3, refractive index $n = 1.465 \pm 0.004$), synthesized following the microemulsion technique [15]. A concentrated master suspension in a mixture of water and 50 wt% glycerol ($n = 1.396$) was produced by centrifugation. Samples of lower concentrations were obtained by dilution with known amounts of fluid. Two series of samples with the same volume fractions and the same suspending fluid were prepared. In one of the series, excess salt was removed by de-ionizing with ion exchange resin and adding extra exchange resin to the samples, thus increasing the range and strength of the direct interaction [1,2]. The other series of samples remained non-de-ionized. The samples were sealed in cylindrical thin-walled glass capillaries with a diameter of 2 mm.

DXS and CCDLS measure the time- and wave-vector-dependent intensity correlation function of coherent radiation scattered by the sample, characterizing the dynamics. DXS was performed at beam line ID10A of the European Synchrotron Radiation Facility in Grenoble [16]. The sample was illuminated with radiation at a wavelength $\lambda = 1.51$ Å. The longitudinal coherence length was about 1 μm. The transverse coherence length was 140 μm vertically and 14 μm horizontally. A pinhole with a diameter of 20 μm was inserted to provide a collimated and partially coherent beam. A scintillation counter served as detector. Intensity correlation functions were computed with an ALV5000/E correlator.

SAXS measurements, yielding the static scattered x-ray intensity as a function of wave vector q, were done under the same experimental conditions as the dynamic measurements. The static structure factor $S(q)$ was determined by dividing the scattered intensity by the particle form factor, measured on a dilute sample.

In the CCDLS setup, a diode pumped, frequency-doubled Nd:YAG laser ($\lambda = 532$ nm) served as the light source. Two multimode optical fibers, kept at a fixed vertical distance, were used to couple the scattered light into two photomultipliers whose outputs were cross correlated. This way of suppressing multiple scattering has been proposed only recently [17].

Figure 1 shows typical intermediate scattering functions $f(q,t)$, determined with DXS. The intermediate scattering function is obtained from the normalized intensity correlation function, $g(q,t)$, according to $g(q,t) = 1 + \beta^2 |f(q,t)|^2$ [1], where β^2 is an apparatus constant. Correlation functions at the same wave vector are compared for a non-de-ionized and a de-ionized sample. The correlation

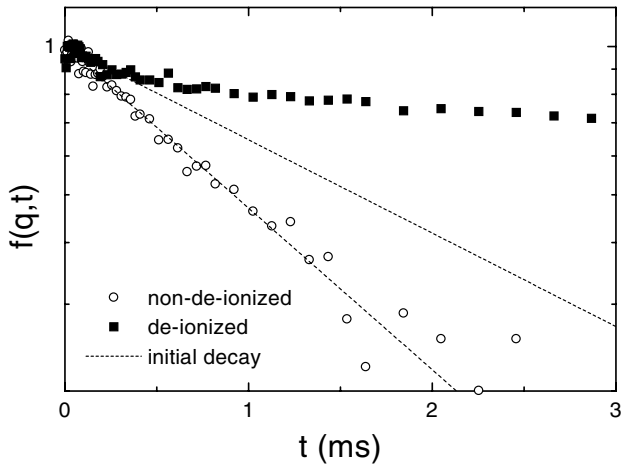

FIG. 1. Intermediate scattering functions, obtained with DXS on suspensions of silica colloids in a mixture of water and glycerol. Non-de-ionized (circles) and de-ionized samples (squares) are compared. The volume fraction $\phi = 0.089 \pm 0.002$. The scattering vector $q = 0.0378$ nm^{-1}. The straight lines represent the initial decay of $f(q,t)$.

functions of the de-ionized samples are less exponential and their initial decay is slower (at this wave vector) as compared to the non-de-ionized samples. This behavior indicates that, although the nominal volume fraction is the same, the system becomes effectively more dense as the range of the direct interaction increases [2].

The initial decay of $f(q,t)$ gives the collective short-time diffusion coefficient according to $D(q) = -\Gamma(q)/q^2$, where $\Gamma(q) = \lim_{t\to 0}[d \ln f(q,t)/dt]$ is the first cumulant [1]. Figure 2 shows the inverse of the short-time diffusion coefficient and the static structure factor for a de-ionized suspension (volume fraction $\phi = 0.089 \pm 0.002$). The diffusion coefficient was divided by that for a dilute sample D_0, measured with dynamic light scattering. De-ionizing the samples leads to an increase of the peak height of both

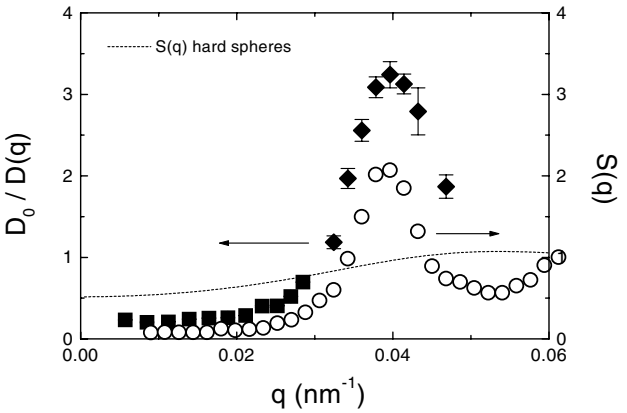

FIG. 2. Inverse of the short-time collective diffusion coefficient (squares CCDLS, diamonds DXS) and static structure factor (circles) for de-ionized silica colloids in water glycerol. The volume fraction $\phi = 0.089$. The diffusion coefficient is scaled by that of a dilute suspension, D_0. The dashed line represents a Percus-Yevick hard-sphere calculation for the structure factor [1].

$D_0/D(q)$ and $S(q)$, a decrease of the osmotic compressibility [$\propto S(q = 0)$], and a shift of the peak to smaller q values with respect to non-de-ionized samples. The shift of the peak indicates an increase of the range of the direct interaction [1]. For comparison, the dashed line in Fig. 2 shows a calculated hard-sphere structure factor for the same volume fraction. The inverse of the diffusion coefficient mimics the q dependence of the structure factor. This behavior is incorporated in the well-known expression [1]

$$D(q) = D_0 H(q)/S(q), \tag{1}$$

where the function $H(q)$ represents the hydrodynamic interactions. Quantitative differences between $D_0/D(q)$ and the structure factor, evident from Fig. 2, indicate that hydrodynamic interactions play an important role.

In Fig. 3 we show $H(q)$ at a representative volume fraction ($\phi = 0.089$). Figure 3(a) shows data on a non-de-ionized sample, and Fig. 3(b) on a de-ionized sample. Qualitatively, the hydrodynamic interaction behaves similarly to hard-sphere-like systems [10]: $H(q)$ is smaller than 1 for all wave vectors, indicating a hydrodynamic hindrance of diffusion. This effect is largest at small q. The experimental curves are compared to the fluctuation expansion theory [9] (dashed lines), taking the measured structure factor as input for the calculations. Since at higher volume fractions many-body effects are expected to be important, the elaborate fluctuation expansion approach should be used [2,14]. For the non-de-ionized samples, reasonable agreement with the theory is found, in accordance with previous results on non-de-ionized silica systems [13]. However, small systematic deviations are apparent: $H(q)$ shows less structure than expected from the calculation. As the samples are de-ionized, these deviations become large, revealing two essential differences to the hard-sphere case: The maximum value of $H(q)$ is much smaller and the q dependence substantially less pronounced than theoretically expected [Fig. 3(b)].

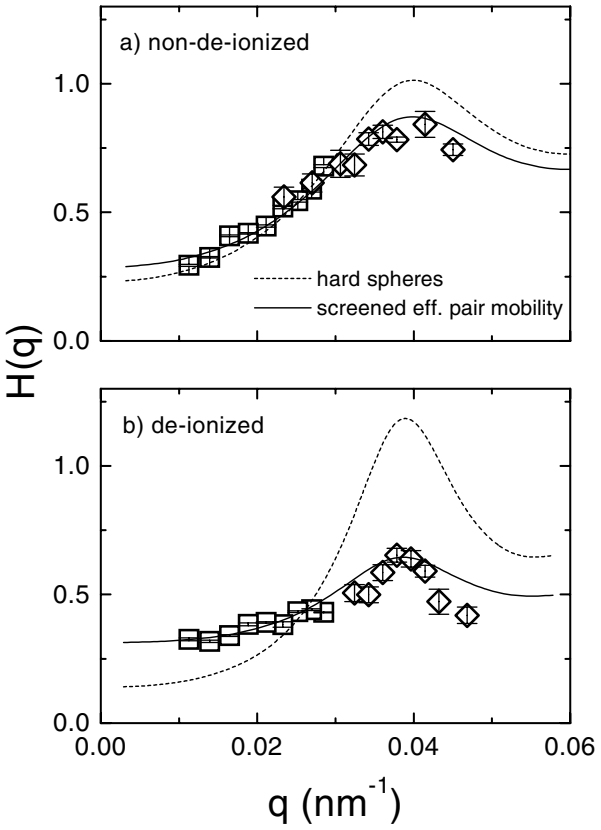

FIG. 3. Hydrodynamic function for silica colloids in a mixture of water and glycerol: (a) non-de-ionized and (b) de-ionized. The volume fraction $\phi = 0.089$ in both cases. CCDLS (squares) and DXS (diamonds) results are shown. The dashed curves represent calculations with the theory by Beenakker and Mazur [9]. The solid lines represent calculations with a screened effective hydrodynamic pair mobility [Eq. (4)].

Since the fluctuation expansion theory cannot describe our data, we now resort to a phenomenological description in terms of an *effective* hydrodynamic pair interaction. To this end, the hydrodynamic function is approximated by

$$H(q) = \mu^* 6\pi\eta_0 a\left(1 + \frac{1}{(2\pi)^3}\int d\mathbf{q}'\,\hat{\mathbf{q}}\cdot\mathbf{A}(\mathbf{q}')\cdot\hat{\mathbf{q}}[S(|\mathbf{q}-\mathbf{q}'|) - 1]\right), \tag{2}$$

where $\hat{\mathbf{q}}$ is a unit vector, a the particle radius, and η_0 the viscosity of the suspending fluid. The function $\mathbf{A}(\mathbf{q})$ represents the leading far-field terms of the effective pair mobility. In the absence of hydrodynamic screening, we have [9,18]

$$\mathbf{A}(\mathbf{q}) = \tfrac{4}{3}\pi a^3 \tfrac{9}{2}(1 - \hat{\mathbf{q}}\hat{\mathbf{q}})\left[\frac{1}{(aq)^2} - \tfrac{1}{3} + O(q^2)\right]. \tag{3}$$

The first term in the square brackets in Eq. (3) is dominant for $q \to 0$ and represents the long-range Oseen term in real space, which decays with the inverse of the interparticle distance ($\propto 1/R$). The following terms represent the dipole contribution ($\propto 1/R^3$). For hard spheres, the prefactor $\mu^* 6\pi\eta_0 a = \eta_0/\eta^*$, where η^* is to linear order in the volume fraction identical to the effective viscosity of the suspension [9]. In analogy to porous media [7], we introduce hydrodynamic screening into the model by substituting

$$\frac{1}{(aq)^2} \to \frac{1}{(aq)^2 + (a/l_{\mathrm{scr}})^2} \tag{4}$$

in Eq. (3). This substitution leads to a sum of exponentially screened terms and a dipolelike interaction in real space, with screening length l_{scr} [7]. In order to adjust the absolute value of $H(q)$, we take the $q = \infty$ limit of the effective mobility, μ^*, as a free parameter. The solid lines in Fig. 3 represent numerical calculations with the screened form of $\mathbf{A}(\mathbf{q})$. Again, the measured structure factor has been used to perform the ensemble average. Screening clearly leads to a flattening of the hydrodynamic function, in good agreement with the experiment.

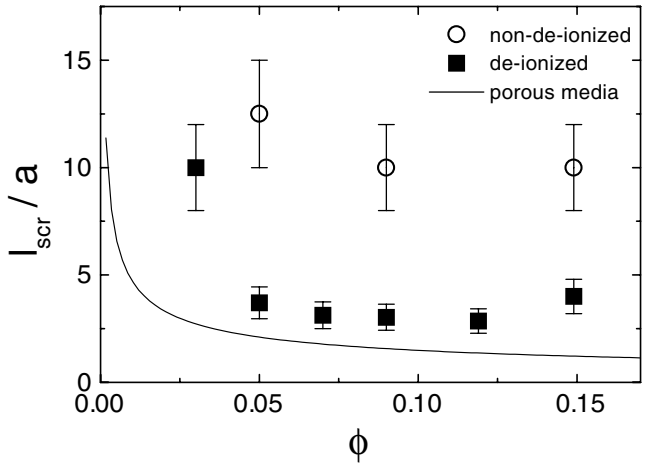

FIG. 4. Hydrodynamic screening length for suspensions of silica colloids, non-de-ionized (circles) and de-ionized (squares). The solid line represents the hydrodynamic screening length for porous media [7].

For the non-de-ionized samples hydrodynamic screening is weak (screening length $l_{\rm scr} \approx 10a$). Furthermore, we find $\mu^* 6\pi\eta_0 a \approx \eta_0/\eta(\phi)$ for these samples, where $\eta(\phi)$ is the viscosity of a hard-sphere suspension at volume fraction ϕ [19]. We conclude that the data for non-de-ionized samples are well described by particles interacting by a slightly screened effective hydrodynamic pair interaction in a fluid of viscosity $\eta(\phi)$, which is still close to the behavior of hard spheres. The essential difference to hard spheres and to previous results on charged suspensions [2,12,13] is, however, the introduction of an effective hydrodynamic screening. Strikingly, hydrodynamic screening is much more pronounced for the de-ionized samples, as is evident from Fig. 3(b). In order to describe the flattening of the data as compared to the hard-sphere theory, a screening length of about 3 particle radii is needed [solid line in Fig. 3(b)]. The mobility μ^*, fixing the absolute value of $H(q)$, becomes much smaller than for the non-de-ionized samples.

In Fig. 4 we show the hydrodynamic screening length for both non-de-ionized and de-ionized systems as a function of volume fraction. At all volume fractions, the screening length becomes substantially shorter as the samples are de-ionized. This result indicates a strong coupling of hydrodynamic and direct interactions. For comparison, the solid line in Fig. 4 shows the hydrodynamic screening length found in effective-medium theories for porous media [6,7], where the solid frame remains *fixed*. It appears that $l_{\rm scr}$ approaches this result as the samples are de-ionized, whereas screening vanishes in the hard-sphere limit. This suggests the following interpretation: the strong Coulomb interaction prevents the particles from moving freely in response to the hydrodynamic field, leading to an effective screening similar to porous media.

From Fig. 1 it is seen that the intermediate scattering function exhibits a slow decay at large times in the de-ionized case. In order to analyze the full nonexponential shape of the correlation functions, the hydrodynamic interaction, obtained from the initial decay, as well as the structure factor is needed as input [20]. This will be the subject of future work.

We thank Judith Wijnhoven for the preparation of the colloidal spheres and Ad Lagendijk for encouragement and discussions. This work has been supported by the "Stichting voor Fundamenteel Onderzoek der Materie (FOM)," which is financially supported by the "Nederlandse Organisatie voor Wetenschappelijk Onderzoek (NWO)."

[1] P. N. Pusey, in *Liquids, Freezing and the Glass Transition,* edited by J. P. Hansen, D. Levesque, and J. Zinn-Justin (Elsevier, Amsterdam, 1991).
[2] G. Nägele, Phys. Rep. **272**, 215 (1996).
[3] B. Cichocki and B. U. Felderhof, J. Chem. Phys. **94**, 556 (1991); **94**, 563 (1991).
[4] A. J. C. Ladd, Phys. Rev. Lett. **76**, 1392 (1996); P. N. Segrè, E. Herbolzheimer, and P. M. Chaikin, Phys. Rev. Lett. **79**, 2574 (1997).
[5] D. L. Koch and E. S. G. Shaqfeh, J. Fluid Mech. **224**, 275 (1991); M. P. Brenner, Phys. Fluids **11**, 754 (1999).
[6] P. J. Mucha, I. Goldhirsch, S. A. Orszag, and M. Vergassola, Phys. Rev. Lett. **83**, 3414 (1999).
[7] L. Durlofsky and J. F. Brady, Phys. Fluids **30**, 3329 (1987).
[8] M. Muthukumar, J. Chem. Phys. **107**, 2619 (1997).
[9] C. W. J. Beenakker and P. Mazur, Physica (Amsterdam) **120A**, 388 (1983); Physica (Amsterdam) **126A**, 349 (1984).
[10] P. N. Segrè, O. P. Behrend, and P. N. Pusey, Phys. Rev. E **52**, 5070 (1995).
[11] U. Genz and R. Klein, Physica (Amsterdam) **171A**, 26 (1991).
[12] W. Härtl, Ch. Beck, and R. Hempelmann, J. Chem. Phys. **110**, 7070 (1999).
[13] A. P. Philipse and A. Vrij, J. Chem. Phys. **88**, 6459 (1988).
[14] G. Nägele, O. Kellerbauer, R. Krause, and R. Klein, Phys. Rev. E **47**, 2562 (1993).
[15] F. J. Arriagada and K. Osseo-Asare, in *The Colloid Chemistry of Silica,* edited by H. E. Bergna (American Chemical Society, Washington, DC, 1994).
[16] G. Grübel and D. L. Abernathy, Proc. SPIE Int. Soc. Opt. Eng. **3154**, 103 (1997).
[17] M. V. Meyer *et al.,* Appl. Opt. **36**, 7551 (1997).
[18] P. Mazur and W. van Saarloos, Physica (Amsterdam) **115A**, 21 (1982).
[19] E. G. D. Cohen, R. Verberg, and I. M. de Schepper, Physica (Amsterdam) **251A**, 251 (1998); A. J. Banchio, G. Nägele, and J. Bergenholtz, J. Chem. Phys. **111**, 8721 (1999).
[20] G. Nägele and P. Baur, Physica (Amsterdam) **245A**, 297 (1997).